Nondestructive Prediction of Fire Performance in Fire Retardant-treated Wood Using X-ray Computed Tomography

Masumi Hasegawa,[a,*] Hiroyuki Okamura,[b] and Yasushi Hano [b]

The fire performance of fire retardant-treated wood can be evaluated based on how much of the chemical retardant is used. Therefore, methods for identifying chemical content in wood are needed. Stereo images of wood samples before and after the fire retardant treatment were captured using micro-focus X-ray computed tomography. Image brightness values, indicating concentration, were calculated using binarized images sliced from the X-ray images. Changes in integrated brightness values before and after treatment showed a strong positive correlation with chemical content at a 1% significance level. The chemical content of the retardant-treated wood was predicted based on the relationship between the two. The predicted values were in agreement with the values measured using the leaching method. Fire performance tests of the fire retardant-treated wood were conducted using a cone calorimeter. The treated wood was classified as fire-retardant and non-combustible wood. In addition, the fire performance predicted by the relationship between changes in integrated brightness values and chemical content agreed with the classification by the fire performance test. These findings suggest that X-ray computed tomography can be potentially used to predict the chemical content of fire retardant-treated wood.

DOI: 10.15376/biores.17.4.6900-6909

Keywords: Fire performance; Fire-retardant wood; Chemical content; X-ray computed tomography; Nondestructive evaluation

Contact information: a: Department of Agro-Environmental Sciences, Faculty of Agriculture, Kyushu University, 744 Motooka Nishi-ku Fukuoka, Japan; b: Interior Design Research Institute, Fukuoka Industrial Technology Center, 3-405 Agemaki Okawa, Japan;
** Corresponding author: kmgtmsm@agr.kyushu-u.ac.jp*

INTRODUCTION

After the revision of the Japanese building standard law, new legislation that promotes wood use in public buildings was enacted in 2010 (Forestry Agency 2010). This has led to an increase in the use of wooden materials in Japan, and approximately 87% of the public buildings in 2019 integrated wooden structures (Forestry Agency 2020). As per the standard building law, it is necessary for such structures to use fire-retardant materials in walls and ceilings. Furthermore, fire retardant-treated wood must have its fire performance accredited by the Ministry of Land, Infrastructure, Transport, and Tourism (MLIT 2011). According to the ISO 5660-1 (2015) standard, the fire retardant-treated wood can be categorized as noncombustible, quasi-noncombustible, or fire-retardant *via* a fire performance test using a cone calorimeter. However, installation of a cone calorimeter can be costly for wood factories. Generally, these factories evaluate the fire performance of fire-retardant wood through the degree of chemical content, which depends on the type

of chemical. Harada *et al.* (2003) demonstrated *via* a cone calorimeter that chemical contents of polyphosphatic carbamates of 80 and 160 kg/m^3 ensured sufficient performance of fire-retardant and achievement of quasi-noncombustible woods, respectively. Nevertheless, some fire-retardant woods with no documented fire performance are occasionally sold on the market. Consequently, it is important to determine whether the required amount of fire-retardant chemical is present in all sections of a wood sample. However, chemical content typically is calculated from the weight difference in samples before and after chemical impregnation; thus, it is difficult to determine the degree of chemical content within an individual sample. The development of non-destructive measurement systems for chemical content in fire retardant-treated wood has attracted considerable attention in the wood industry. Hasegawa *et al*. (2017) evaluated chemical content in fire retardant-treated wood using an air-coupled ultrasonic method. They reported that the relative changes in ultrasonic wave velocity had a positive correlation with chemical content. However, this technique is not sufficient for evaluating the distribution of chemical content over the thickness.

X-ray computed tomography (X-ray CT) is a technique that allows non-destructive reconstruction of the 3D internal structure of objects without any prior preparation (Thompson and Leach 2018). In the field of wood science, X-ray CT is used to measure wood properties, such as density, moisture content, and internal features (Wei *et al.* 2011; He and Qi 2013; Li *et al.* 2013; Krähenbühl *et al.* 2014; Li *et al.* 2018). He and Qi (2013) accurately predicted the density and moisture content of *Larix gmelinii* using a regression formula calculated from the X-ray CT data. Li *et al.* (2013) evaluated the moisture content using grayscale values obtained from X-ray CT data. They reported that the method is accurate and has excellent potential for the non-destructive measurement of the moisture content distribution in 3D. Li *et al*. (2018) reported that X-ray CT is valuable for periodically visualizing internal structural changes and monitoring water distribution in medium-density fiberboard and oriented strand board during water sorption.

In this study, the authors attempted to investigate the non-destructive prediction of the fire performance of fire retardant-treated wood using sliced images captured by X-ray CT. First, the relationship between chemical content in fire retardant-treated wood and integrated brightness values obtained by X-ray CT was determined. Second, the distribution of chemical content was predicted using X-ray CT. Finally, the chemical content was evaluated *via* cone calorimetry and compared to the predicted values.

EXPERIMENTAL

Materials

Kiln-dried sapwood of Japanese cedar (*Cryptomeria japonica*) was used as the test material. Three samples were prepared from the lumber, as illustrated in Fig. 1, which were used in two experiments. Sample S1 was used in the first experiment, and S2 and S3 were used in the second experiment. S1 was cut into six test samples with dimensions of 200 mm × 30 mm × 20 mm. Six test samples were divided into one piece per concentration. After X-ray photography, S1 was cut into five test samples, as shown in Fig. 1. These samples were used to measure the chemical content (CC) using the leaching method. S2 and S3 were cut into four test samples (SN-1, SN-2, SN-3, SN-4, N = 2, 3) with dimensions of 100 mm × 100 mm × 20 mm, as shown in Fig. 1. Four samples, S2-1, S2-2, S3-1, and S3-2, were used for the fire performance test using a cone calorimeter. Other test samples,

S2-3, S2-4, S3-3, and S3-4, were used to measure the CC using the leaching method. The average air-dried density of each sample was 360 kg/m^3.

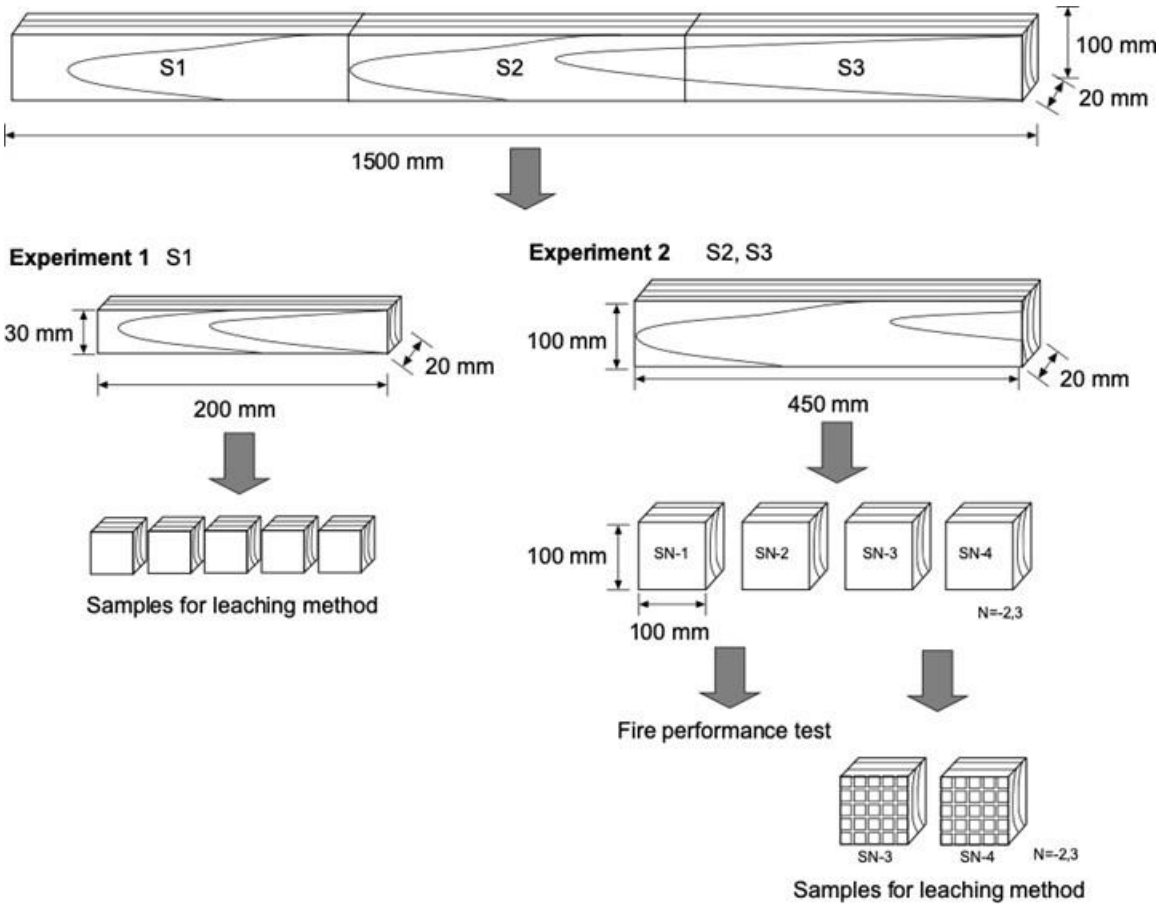

Fig. 1. Illustration of the wood test samples

Treatment with Fire-retardant Solution

A commercial fire retardant, whose main component is guanidine phosphate, was used to impregnate the wood samples. The fire retardant was diluted with distilled water so that the weight ratio of the solid content was 0%, 10%, 20%, 30%, 40%, and 50% for the first experiment, and 20% and 50% solutions for the second experiment. Samples were placed in a vacuum desiccator at -0.09 MPa for 2 h, and subsequently, dipped into the retardant solutions and placed in a vacuum desiccator at 0.7 MPa for 2 h. After impregnation, samples were air-dried for three weeks and then dried in a constant-temperature oven at 60 °C to a constant weight.

Calculation of Chemical Content

The chemical content of the total sample (C_T) was calculated using Eq. 1,

$$C_T = (W_a - W_b) / V_T \quad (1)$$

where W_a is the sample weight (kg) after chemical impregnation and drying at 60 °C for 24 h, W_b is the weight (kg) of the sample dried at 60 °C for 24 h before chemical impregnation, and V_T is the volume (m^3) of the sample before chemical impregnation.

Finally, the samples for the first and second experiments were cut into 5 and 25 measurement areas, respectively, as shown in Fig. 1. Chemical content of the measurement

area was measured using the leaching method. Samples were dipped into distilled water and placed in a vacuum desiccator at -0.9 MPa for 24 h. Then, the weight of the samples was measured, and the samples were again dipped into distilled water and placed in the vacuum desiccator. This operation was continued until a constant sample weight was obtained. After leaching, samples were air-dried for three weeks and then dried in a constant-temperature oven at 60 °C to a constant weight. The chemical content (C_L) was calculated using Eq. 2,

$$C_L = (W_{Lb} - W_{La}) / V_L \quad (2)$$

where W_{La} represents the sample weight (kg) after leaching, chemical impregnation, and drying at 60 °C for 24 h, W_{Lb} is the weight (kg) of the sample dried at 60 °C for 24 h before leaching, and V_L represents the volume (m^3) of the sample after leaching.

X-ray Computed Tomography

X-ray images of the rotated samples were captured using a micro-focus computed tomography device (MCT225K, Nikkon Solutions Co., Ltd., Tokyo, Japan). The captured images were used to reconstruct the 3D shape data of the samples. The X-ray source was set to a minimum focus of 3 µm, 16 bit; and flat-panel detector was set to 4M pixel resolution. The tube voltage and electric current were set to 130 kV and 160 µA, respectively. The source image receptor distance (distance between the X-ray source and detector) and source to object distance (distance between the X-ray source and sample) were 1175 and 724 mm, respectively. The number of captured images was 1200 sheets during photography. The 3D shape data were constituted in 8G voxels (0.125 mm, 32 bits). The 3D shape data were then sliced into 16-bit images at 0.125 mm intervals using VGStudioMax 2.2 (Volume Graphics Ltd., Heidelberg, Germany). Brightness values were calculated from the sliced images using Image J 1.47 (NIH, Bethesda, MD, USA). The integrated brightness values for the measurement areas of samples from the two experiments were calculated by multiplying the brightness values integrated in the thickness direction of each measurement area by the total number of pixels.

Fire Performance Test

Fire performance tests of the fire-retardant-treated wood were conducted using a cone calorimeter in accordance with the ISO 5660-1 (2015) standard. The heat release rate (HRR), total heat release (THR), and surface conditions, such as holes and cracks, were used to determine the types of fire performance of wood. The following standards were used: (1) THR must be 8 MJ/m^2 or less, in 5 min for fire-retardant, 10 min for quasi-noncombustible, and 20 min for noncombustible materials; (2) HRR must not exceed 200 kw/m^2 in 10 s.

RESULTS AND DISCUSSION

Relationships between Brightness Values and Chemical Content

Table 1 lists the chemical content (CC) of the samples with various concentrations of the retardant chemical and the corresponding densities. The total CC (C_T) was similar to the average CC (C_L). The CC increased with an increase in chemical concentration. After chemical impregnation, density increased with increasing CC. Figure 2 shows gray-scaled images at the center and edge of the samples before and after chemical impregnation for

different chemical concentrations. The reduced shade represents latewood, which has a large density, and the deep color represents earlywood, which has a low density. The annual rings constitute earlywood and latewood. The density of earlywood is lower than that of latewood because of the difference in lumen diameter and cell wall thickness (Kollmann and Cote 1967). As a result, annual rings can be described using the difference in grayscale color. The reduced shade area after chemical impregnation was larger than the shade area before impregnation. Density of the samples increased because of the increase in content of solid component of the fire retardant.

Table 1. Chemical Content (Total and Average) and Density (Before and After Chemical Impregnation) for Samples with Different Chemical Concentrations of the Retardant

Chemical Concentration (%)	Chemical Content (kg/m^3)		Density (kg/m^3)	
	C_T	C_L	Before	After
0	0	2	346	345
10	37	37	363	370
20	76	73	365	421
30	121	115	339	459
40	184	174	353	513
50	213	200	356	535

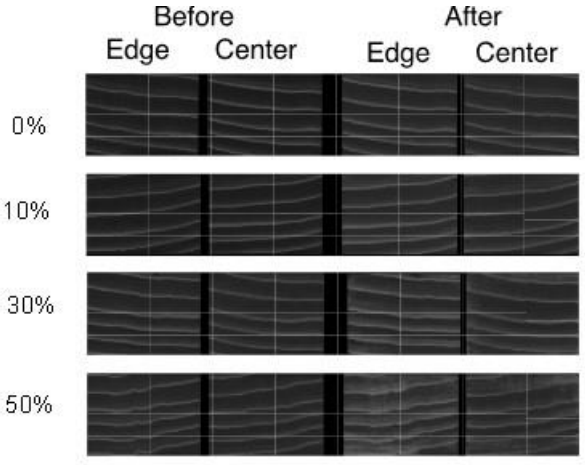

Fig. 2. Images of sample cross-sections captured by X-ray CT

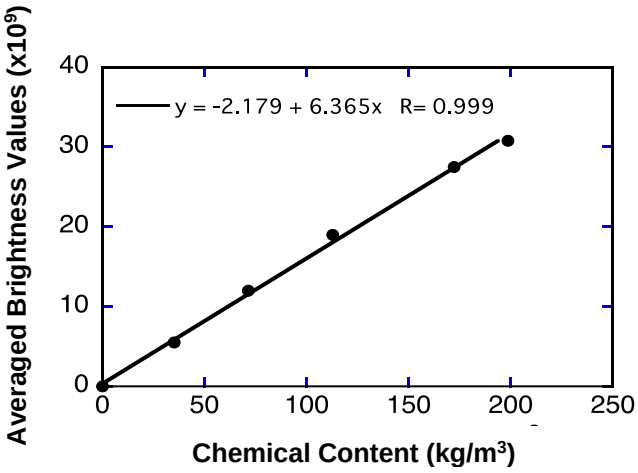

Fig. 3. Relationship between chemical content and averaged brightness values for different chemical concentrations

Figure 3 shows the relationship between the changes in the integrated brightness value and the CC of the samples. The change in the integrated brightness value exhibited a significant positive correlation with the CC ($p < 0.001$). These results suggest that it is possible to predict the chemical distribution in fire-retardant-treated wood by analyzing the X-ray CT images.

Expression for Prediction

Figure 4 shows a positive correlation between CC (C_L) and changes in brightness values for the samples S2-4 and S3-4 treated with 20% and 50% chemical concentrations ($p < 0.001$). Based on this result, an expression for prediction was obtained. The CCs of S2-3 and S3-3 were predicted using the expression shown in Fig. 4. As shown in Fig. 5, the predicted CCs had positive correlations with the measured CCs (C_L) at the 0.1% significance level. Figure 6 illustrates the distributions of the predicted CC of samples treated with 20% and 50% concentrations of the chemical retardant (S2-1, S2-2, S3-1, and S3-2). The predicted CCs were higher in the outer layers of the sample than in the inner layers. This could be attributed to the fact that during the drying process of the impregnated samples, the solid component of the water-soluble retardant moved to the edges of samples together with water. Therefore, water evaporated, but the solid component remained concentrated at the edges. Takase *et al*. (2019) reported that different drying conditions after chemical treatment can produce fire retardant-treated wood with uneven chemical distribution. Table 2 shows the predicted CCs for S2-1, S2-2, S3-1, and S3-2. The CCs of S2 and S3 ranged from 76 to 135 kg/m^3 and 160 to 430 kg/m^3, respectively; their average CCs were 101 and 258 kg/m^3, respectively.

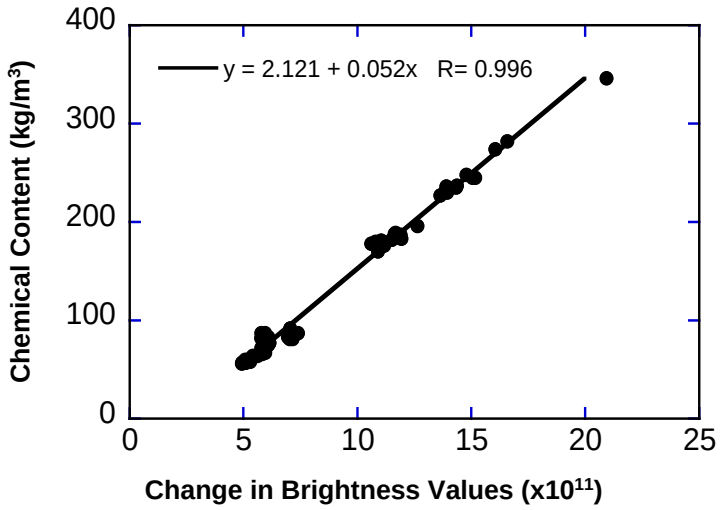

Fig. 4. Relationship between chemical content and changes in brightness values

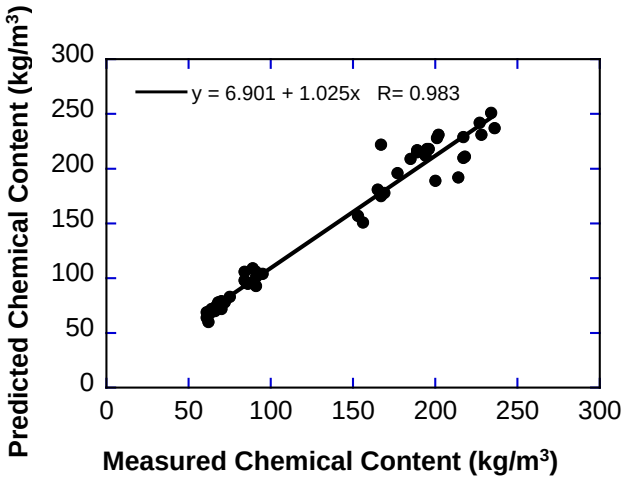

Fig. 5. Relationship between the measured and predicted chemical contents

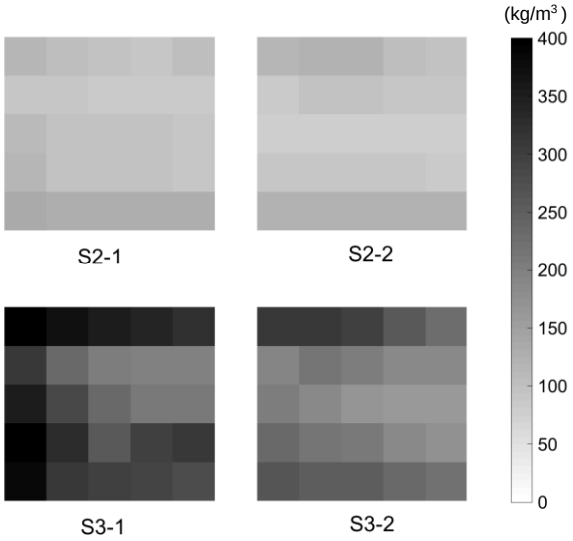

Fig. 6. Distributions of predicted fire-retardant chemical

Table 2. Predicted Chemical Content and Classification of Fire Performance

Sample	Chemical Concentration (%)	Chemical Content (kg/m^3)			Classification	
		Average	Maximum	Minimum	Prediction	Cone Calorimeter
S2-1	20	103	135	87	Fire-retardant	Fire-retardant
S2-2		99	125	76		
S3-1	50	296	430	198	Noncombustible	Noncombustible
S3-2		220	311	160		

Harada *et al.* (2003) used a cone calorimeter to determine the fire performance of wood samples treated with phosphoric acid-based chemicals. The test identified the CC criteria at 80 and 160 kg/m^3, for fire-retardant wood and quasi-noncombustible wood, respectively. According to these criteria, the impregnated samples (S2 and S3) were predicted as fire-retardant and noncombustible wood, respectively.

Fire Performance Test

After the cone calorimeter test, some cracks appeared, but no holes were found in the samples. The appearance had no difference between test samples treated with 20% and 50% chemical concentrations. Figure 7(a) shows the HRR curves. In S2, the HRR values went up suddenly at 5 min and peaked at 10 min. After reaching the peaks, HRR plunged and remained constant. However, in S3, the HRR values increased gradually. Generally, untreated wood shows a rapid increase in HRR immediately after the test start, then it decreases and increases again (Harada *et al*. 2003). Harada and Kamikawa (2010) conducted the fire performance test of Japanese cedar using a cone calorimeter test. The maximum HRR and THR in 15 minutes of wood samples without a fire retardant were 124 and 63 MJ/m^2, respectively. In this study, the HRR of S2 and S3 samples gradually increased within 5 min of the test start due to the fire retardant impregnation. The phosphorus-nitrogen-based fire retardant used in this study had two effects: 1) it generated intumescent carbonized layers that suppressed the amount of oxygen supply; 2) it released the inert nitrogen gas that diluted the combustible gas (Ishihara 1989; Lowden and Hull 2013). Consequently, this fire retardant provides high fire performance for the treated wood. Figure 7(a) supports this hypothesis of the effect of fire retardant.

Figure 7(b) shows the THR curves. The THR of sample S2 exceeded 8 MJ/m^2 within 10 min. However, the THR of S3 did not go beyond 8 MJ/m^2 within 20 min. These results indicated that S2 and S3 samples were fire-retardant and noncombustible wood, respectively. The classification of the chemical content of the samples was in agreement with that of the cone calorimetric test. These findings suggest that it is possible to predict the fire performance of fire retardant-treated wood *via* X-ray CT.

In this study, the authors evaluated the fire performance of fire retardant-treated wood in terms of the total chemical content. However, it has been established that the distribution of chemical content over the sample thickness also affects the fire performance. Takase *et al*. (2019) investigated the fire performance of fire retardant-treated wood with different chemical distributions using a cone calorimeter. Wood with a high distribution of chemical in the front of the fire testing surface showed a THR up to 20 min was equal to or less than that of the uniformly treated wood. Thus, it is important to consider the chemical distribution over the thickness in a fire performance test, which the authors will attempt to investigate using micro-focus X-ray CT in future research.

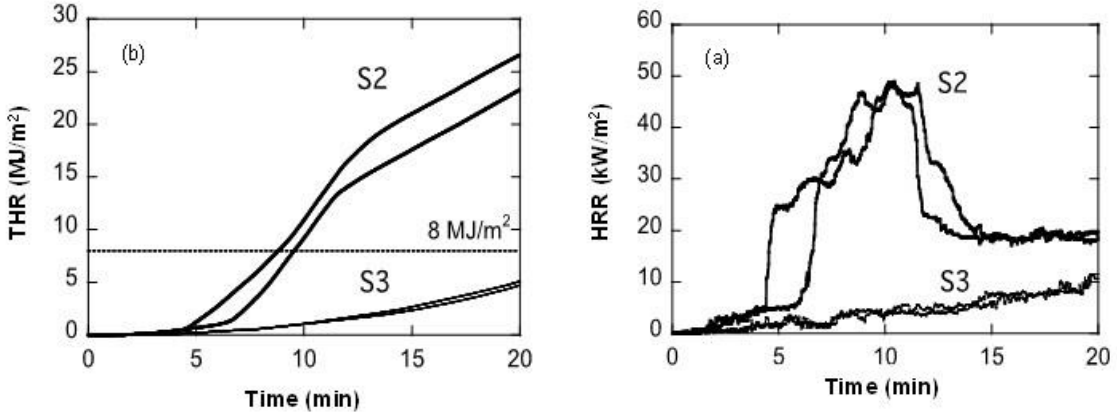

Fig. 7. Changes of (a) heat release rate and (b) total heat release

CONCLUSIONS

1. Changes in integrated brightness values showed a strong positive correlation with the chemical content ($p < 0.001$).
2. Chemical content obtained using a prediction expression agreed with the chemical content measured with leaching method.
3. Classification of fire performance predicted by the chemical content agreed with the classification by a cone calorimeter test. Nondestructive prediction of fire performance in fire retardant-treated wood will be required to consider the chemical distribution over the thickness in the future research.

ACKNOWLEDGMENTS

This work was supported by JSPS KAKENHI, Grant No. 21K04353.

REFERENCES CITED

Forestry Agency (2020). *Annual Report on Forest and Forestry in Japan*, Ministry of Agriculture, Forestry and Fisheries, Japan, Tokyo, Japan.

Forestry Agency (2010). *Legislation for the Promotion of Wood Use in Public Buildings*, Ministry of Agriculture, Forestry and Fisheries, Japan, Tokyo, Japan.

Harada, T., and Kamikawa, D. (2010). "Combustibility of wood heated with a low heat flux," *Mokuzai Kogyo* 65(1), 13-18. (In Japanese)

Harada, T., Uesugi, S., and Taniuchi, H. (2003). "Evaluation of fire-retardant wood treated with poly-phosphatic carbamate using a cone calorimeter," *Forest Products Journal* 53(6), 81-85.

Hasegawa, M., Kumamoto, T., Okamura, H., Asakura, R., Takeuchi, K., and Matsumura, J. (2017). "Relationship between chemical retention and velocity of air-coupled ultrasonic waves in fire retardant-treated wood," *BioResources* 12(2), 3387-3395. DOI: 10.15376/biores.12.2.3387-3395

He, X., and Qi, D. (2013). "Density and moisture content forecasting based on X-ray computed tomography," *European Journal of Wood and Wood Products* 71, 647-652. DOI: 10.1007/s00107-013-0722-3

Ishihara, S. (1989). "Combustion of wood and its control," *Mokuzai Gakkaishi* 35, 775-785. (In Japanese)

ISO 5660-1 (2015). "Reaction-to-fire tests -- Heat release, smoke production and mass loss rate -- Part 1: Heat release rate (cone calorimeter method) and smoke production rate (dynamic measurement)," International Organization for Standardization, Geneva, Switzerland.

Kollmann, F. P., and Cote, W. A. (1967). *Principles of Wood Science and Technology I Solid Wood*, Springer-Verlag, Berlin, Germany.

Krähenbühl, A., Kerautret, B., Debled-Rennesson, I., Mothe, F., and Longuetaud, F. (2014). "Knot segmentation in 3D CT images of wet wood," *Pattern Recognition* 47(12), 3852-3869. DOI: 10.1016/j.patcog.2014.05.015

Li, W., Den Bulcke, J. V., Windt, I. D., Van Loo, D., Dierick, M., Brabant, L., and Van Acker, J. (2013). "Combining electrical resistance and 3-D X-ray computed tomography for moisture distribution measurements in wood products exposed in dynamic moisture conditions," *Building and Environment* 67, 250-259. DOI: 10.1016/j.buildenv.2013.05.026

Li, W., Van Den Bulcke, J., Dhaene, J., Zhan, X., Mei, C., and Van Acker, J. (2018). "Investigating the interaction between internal structural changes and water sorption of MDF and OSB using X-ray computed tomography," *Wood Science and Technology* 52, 701-716. DOI: 10.1007/s00226-018-0992-3

Lowden, L. A., and Hull, T. R. (2013). "Flammability behavior of wood and a review of the methods for its reduction," *Fire Science Reviews* 2, article no. 4. DOI: 10.1186/2193-0414-2-4

Ministry of Land, Infrastructure, Transport, and Tourism (MLIT) (2011). "Noncompliance with Ministerial approved specifications for noncombustible materials concerning noncombustible wood," (http://www.mlit.go.jp/report/press/house05_hh_000251.html), MLIT, Accessed 04 July 2022.

Takase, R., Kamikawa, D., Hasemi, Y., and Matsuyama, K. (2019). "Burning characteristics of fire-retardant-treated wood unevenly treated," *Journal of Environmental Engineering, Architectural Institute of Japan*. 84(762), 709-717. (In Japanese) DOI: 10.3130/aije.84.709

Thompson, A., and Leach, R. (2018). "Introduction to industrial X-ray computed tomography," in: *Industrial X-ray Computed Tomography*, S. Carmignato, W. Dewulf, and R. Leach (eds.), Springer, Cham, Switzerland, pp. 1-23. DOI: 10.1007/978-3-319-59573-3

Wei, Q., Lebion, B., and Rocque, A. L. (2011). "On the use of X-ray computed tomography for determining wood properties: A review," *Canadian Journal of Forest Research* 41(11), 2130-2140. DOI: 10.1139/x11-111

Article submitted: August 26, 2022; Peer review completed: October 1, 2022; Revised version received and accepted: October 19, 2022; Published: October 21, 2022.
DOI: 10.15376/biores.17.4.6900-6909